LAWRENCE
LIVERMORE
NATIONAL
LABORATORY

LLNL-TR-635400

HERMES Model Modifications and Applications 2012

J. E. Reaugh

April 17, 2013

Disclaimer

This work performed under the auspices of the U.S. Department of Energy by Lawrence Livermore National Laboratory under Contract DE-AC52-07NA27344.

HERMES MODEL MODIFICATIONS AND APPLICATIONS 2012

John E. Reaugh

Introduction

HERMES was developed to meet requirements for a model to describe explosive response to impacts that do not produce prompt detonation [1, 2–7], but can include delayed detonations such as DDT and XDT. Such response is termed High Explosive Violent Response (HEVR). The HERMES model includes a constitutive description of strength as a function of pressure, strain-rate, strain, and ambient temperature; the development of damage including fragmentation and porosity; the conditions leading to ignition; the propagation of a burning reaction through the volume of damaged explosive; the burn-up of the damaged and undamaged explosive; and the development of detonation using the Computational Reaction Evolution dependent on Entropy (S) and Time (CREST) detonation model [8, 9]. CREST can distinguish gradual pressure increases from shock waves, and also predict the increase in shock sensitivity to detonation that results from increased porosity.

This year HERMES has been implemented as a User Defined Function in ALE 3D. As a result, modifications to the model can be implemented in a timely fashion asynchronously from the ALE 3D distribution process. There are differences between the implementation of HERMES in ALE 3D and the implementation in LS DYNA. The major difference is the propagation of an ignition front from an element that has started to burn. In LS DYNA, the time at which an element begins to burn is based on the minimum line-of-sight distance between the element and any previously ignited element. In ALE 3D the time to burn is based on a level-set method that propagates the ignition front from all elements that were previously ignited. The ALE 3D implementation modifies the time of ignition when element deformation changes the distance from the element to the source. The LS DYNA implementation does not. There are also differences in the implementation of artificial viscosity, which is important for CREST since the artificial viscosity increases the element entropy in a shock. In general, however, the differences have proven minor.

In collaboration with the Atomic Weapons Establishment, UK (AWE), we have characterized two additional explosives – PETN and Composition B, a mixture of 60% RDX and 40% TNT by weight. Applications of HERMES to these explosives are described below.

Application to DDT for HMX

If broken, porous explosive is shocked with sufficient amplitude, a detonation can develop. It is observed for all explosives that for one-dimensional plane shocks, the distance between the surface where a shock was introduced, and the point in the interior of the explosive where detonation develops (run-distance), depends on the shock amplitude. Weaker shocks require a longer run-distance to develop. The CREST model distinguishes shocks from gradual pressure

rises. We have chosen a simple subset of the CREST equations to couple detonation development with the growth of reaction due to burning in broken material. The subset of the CREST reaction model being used is given by:

$$
\begin{aligned}
\dot{\lambda} &= m_2 \lambda_2 (1-\lambda) \\
\dot{\lambda}_1 &= (1-\lambda_1)\sqrt{-2b_1 \ln(1-\lambda_1)} \\
\dot{\lambda}_2 &= \lambda_1 (1-\lambda_2)\sqrt{2b_2\left[\frac{b_2\lambda_1}{b_1} - \ln(1-\lambda_2)\right]} \\
b_1 &= c_0 (Z - c_{13})^{c_1} \\
b_2 &= c_2 (Z - c_{13})^{c_3} \\
m_2 &= \frac{c_{10}}{\sqrt{b_2}} (Z - c_{13})^{c_{11}}
\end{aligned}
\qquad \{1\}
$$

Here we have used the notation of [8]. The Z parameter is a function of entropy as described by [8,9]. The parameter c_{13} may be positive, negative, or zero. (This is a change from the standard CREST model.) The resulting Pop-plots (run distance as a function of shock pressure) exhibit either a cut-off shock pressure (below which a detonation does not form) when c_{13} is positive, or an asymptotic run distance approached at low shock pressure when c_{13} is negative, or a power-law dependence when c_{13} is zero. We refer to this particular subset of the CREST equations as CREST-lite. The HERMES implementation (versions *75a* and higher) includes user-specified upper bounds for the *b*- and *m*- parameters, and an upper bound for the increase in burn fraction, λ, in any cycle. We have also incorporated a special integration for λ_1 when λ_1 is small, so that it may be initialized to zero rather than some small but positive value.

The run-distance to detonation (Pop-plot) for an HMX-based explosive developed at AWE is shown in Figure 1. Calculations were performed using Equation 1 with c_{13} zero. The parameter values were chosen to fit the normal density data. The calculated run distance at 86% density is a prediction. We also show recent (unpublished) data for 86% density HMX powder [10]. The prediction for the higher porosity explosive is more sensitive than the experimental results. We refit the CREST-lite parameters for the reduced density HMX and show those results in Figure 1 as well.

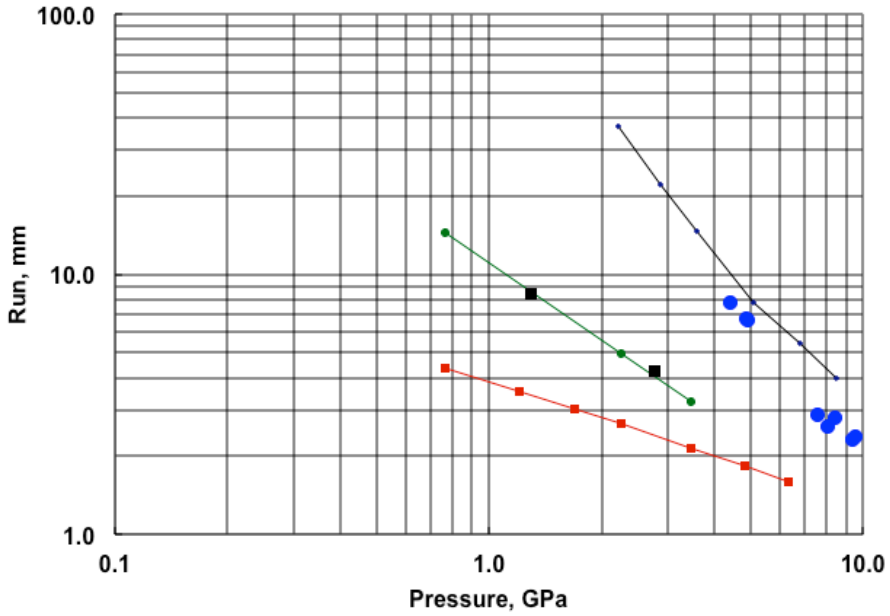

Figure 1: Measured run distance to detonation, mm, as a function of pressure, GPa for 0.3% porosity HMX (solid circles) [11] and 14% porosity (solid squares) [10]. Calculated run distance for formulated HMX explosive with 9% binder but 0.1% porosity (solid black line with dots), the same parameters but for 14% porosity (solid red line with small squares) and new parameters fitted to 14% porosity (solid green line with small circles)

We used the refitted set of parameters to calculate the violence of reaction in Sandusky's DDT apparatus [12]. That apparatus is shown in Figure 2, and the deformation after DDT is shown in that figure as well. At a given time, the height of the maximum inner diameter correlates well with the point of transition. The baseline properties for this calculation of 14% porous HMX are the particle size distribution (1mm diameter spheres) and the propagation velocity of the ignition front away from the ignition plane (200 m/s). For that case, the transition is 210 mm from the ignition plane and occurs at 620 μs. We altered these properties by nominal factors of 2 to determine the sensitivity of our results to these parameters. We found that the location of the detonation transition varies with the square root of the particle diameter, and the time to that transition varies with nearly the first power (0.9) of the particle diameter. Similar changes in the location and time of transition are obtained when the laminar burn speed is changed by a comparable factor. The results were less sensitive to the ignition front velocity. The location of the transition varies with the fifth-root (0.2) of the velocity, and the time to transition varied with the inverse fifth-root of the velocity. We found that the SDT properties were very important. Using parameters for the predicted Pop plot at 14% porosity (red curve of Figure 1) instead of those for the fitted curve (green) reduces the transition distance from 210 mm to 30 mm. We note that increasing the particle diameter to more than 2 mm results in a strong interaction of the developing pressure waves with the end cap of the apparatus, and so confusing the detonation transition location. The compressibility and strength of the porous explosive, which we varied from nil (snowplow model used in other CREST implementations) to the nominal 0.4-GPa crush strength and 0.2-GPa maximum strength, also influence the transition point. In calculations with no strength, the transition point was 40 mm closer to the ignition plane and occurs 80 μs later.

As a result of these sensitivities to properties of the explosive, validating our model (or anyone else's) requires a significant number of independent experiments. Such experiments would be designed to measure the laminar burn speed as a function of pressure, the particle size distribution, the porosity, the resistance to compaction of the porous explosive, the velocity of the ignition front (as a function of pressure, porosity, and permeability), and the Pop plot (run to detonation) as a function of porosity. Few DDT publications report independent measurements of all these properties.

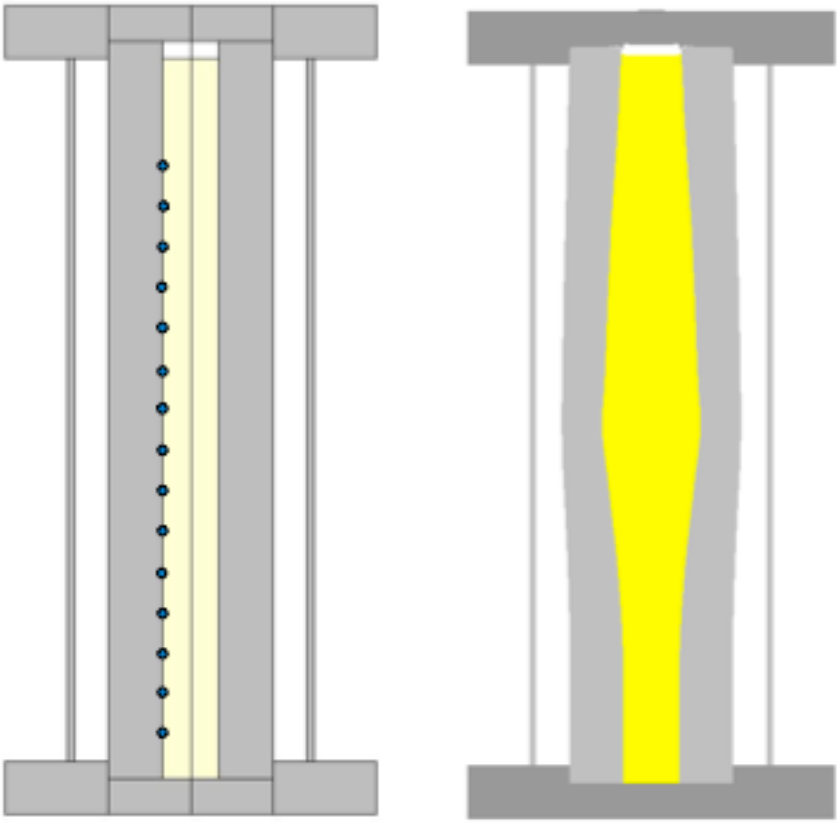

Figure 2: Sandusky apparatus for DDT experiments. The array of calculational gauges is shown schematically on the left. The 340 mm tube has 25mm ID and 25 mm wall thickness. The ignition plane is at the bottom, and a Teflon spacer is at the top of the explosive column. The right-hand side shows the deformation of the apparatus at 740 μs after ignition.

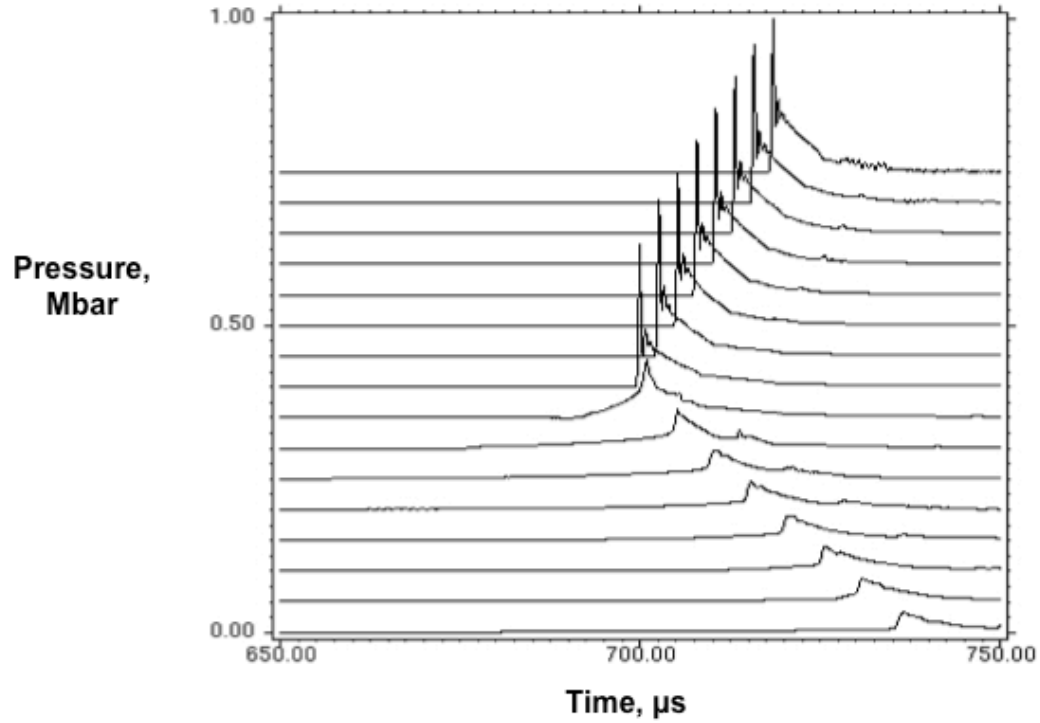

Figure 3: Pressure gauge histories for a DDT. The gauges are stacked so that each 20 mm increase in gauge location is shown displaced by 0.05 Mbar. The fast propagation of a detonation from about the mid-height position propagating to the top is accompanied by a decaying retonation back into the partially burned explosive. Note that the time scale has a suppressed zero, and starts 650 *μ*s after ignition. In this calculation strength has been suppressed.

Applications to SDT for PETN

With the help of AWE colleagues John Curtis and Mary-Ann Maheswaran, we fit SDT parameters to three densities of PETN. At near crystal density, PETN behaves like a homogeneous explosive, rather than a heterogeneous one [13]. For homogeneous explosives, detonation from a shock builds first from the piston, then propagates at faster than normal detonation speed into pre-shocked and denser explosive, then breaking out into undisturbed explosive and slowing to the customary velocity for that density. This is a different mechanism from customary detonation in heterogeneous explosive. We decided to focus on heterogeneous explosives, since that is the behavior observed for HMX and HMX-based explosives as well. The highest density we considered for this study, 1.6 g/cc, behaves as a heterogeneous explosive. The HERMES model uses a tabular equation of state for the gas products, based on Cheetah calculations. As a result, the calculations of the detonation properties of low-density explosives are quite accurate. We illustrate this in Figure 4.

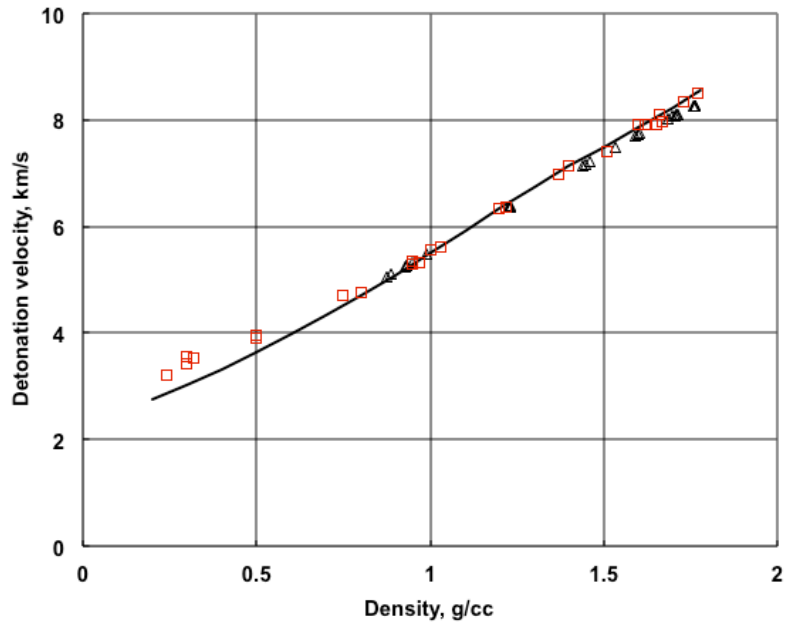

Figure 4: Detonation velocity in PETN as a function of starting density. Measurements from [14] (black triangles) and [15] (red squares). Calculated values from an EOS table developed by Cheetah.

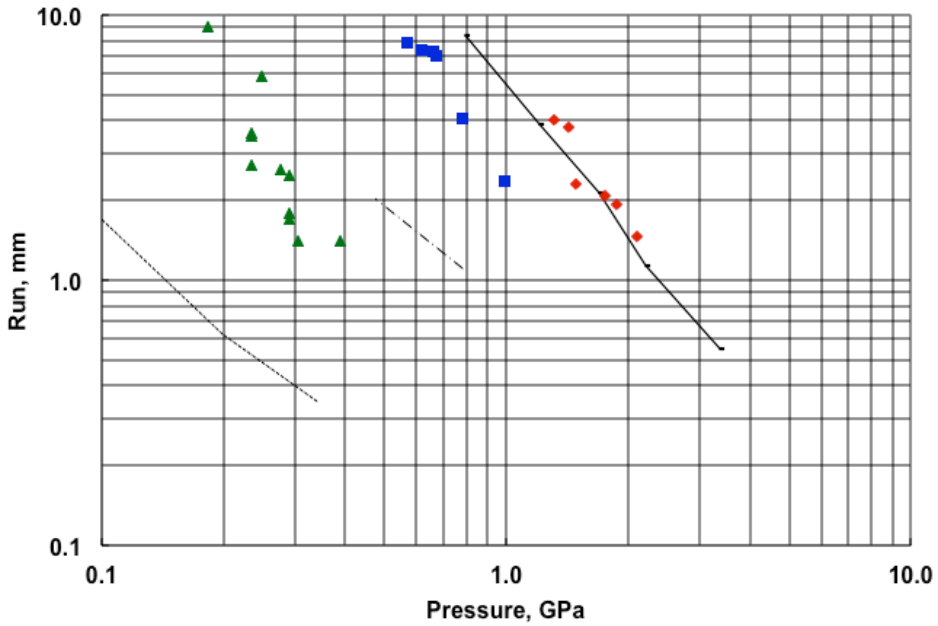

Figure 5: Run distance as a function of shock in the unreacting PETN powder shown for three different powder densities 1.6 (red diamonds) [13], 1.4 (blue squares) [11] and 1.0 (green triangles) [16]. The fitted curve for density 1.6 is also used for the other two densities (dashed and dotted lines). Here, too, the CREST model predicts a more sensitive explosive than is actually measured.

Pop plot data for PETN at three densities is available in the literature. The data for density 1.0 PETN gave values for the shock pressure in the unreacting powders that were stated to be

inaccurate [16]. However, those authors published the free-surface velocity of the brass flyer plate adjacent to the wedge of explosive. As a result, we were able to calculate the unreacted shock pressure as a function of the shock in the brass as determined by the free-surface velocity. These results are given in Figure 5 as well as applications of CREST parameters fit at density 1.6 to the lower density experiments. Work on refitting the lower density data and subsequent application to DDT is ongoing at AWE.

The application of CREST-lite parameters, which have been fit to a given density, to lower-density SDT is seen to result in predictions that are more sensitive than the experimental results for PETN as well as HMX. Other results, not shown here, suggest that this is also the case for Tetryl powders. We do not know why this is the case. A short-term fix, which is being addressed by our AWE colleagues, is to seek a systematic change in the parameter set with porosity. At present, only PETN (and possibly Tetryl, which has little to no programmatic support at either laboratory) enjoys a sufficiently extensive database to support a search for such systematics. A longer term study is based on the hypothesis that there is a different SDT mechanism at work for low density powders, in contrast to the small variations in porosity that result from conventionally pressed parts. The longer term study would develop a new continuum reactive flow model capable of describing and distinguishing the two (or more) mechanisms at work.

Application to Composition B

We had previously developed a mechanical model for Composition B [17], and have somewhat revised that mechanical model and added CREST parameters to fit Pop plot data. The data and fit are shown in Figure 6. We then applied these parameters to a set of experiments using tungsten spheres fired at a disk of Composition B within a tantalum cover plate. The geometry is illustrated in Figure 7. The results for 25 mm sphere at 1 km/s (no go) and 1.25 km/s (go) are shown in Figure 8. Similar results were found for a 10 mm sphere at 2 km/s (no go) and 2.5 km/s (go). This is in accord with the experimental results shown in Figure 9 [18].

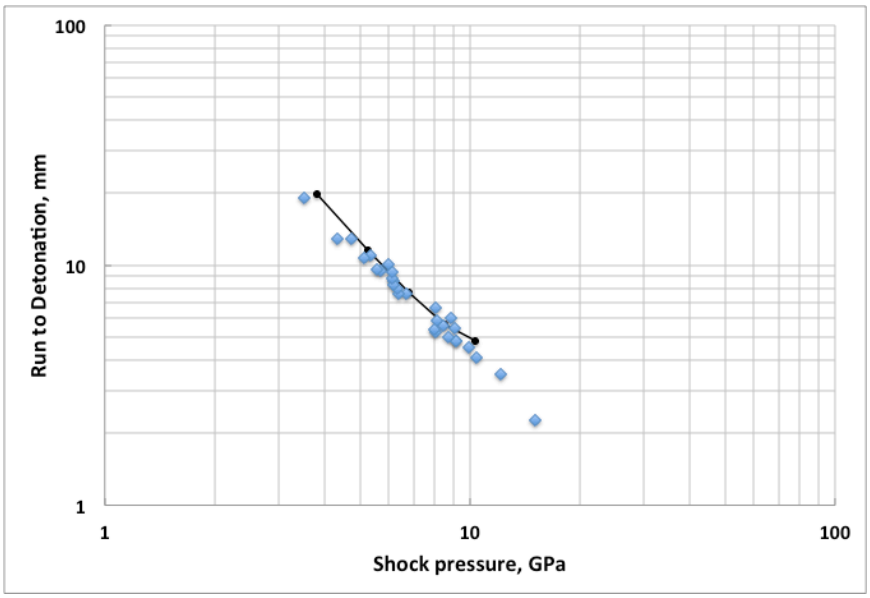

Figure 6: Run distance as a function of shock pressure in Composition B [19]. The solid line is the result of fitting CREST parameters.

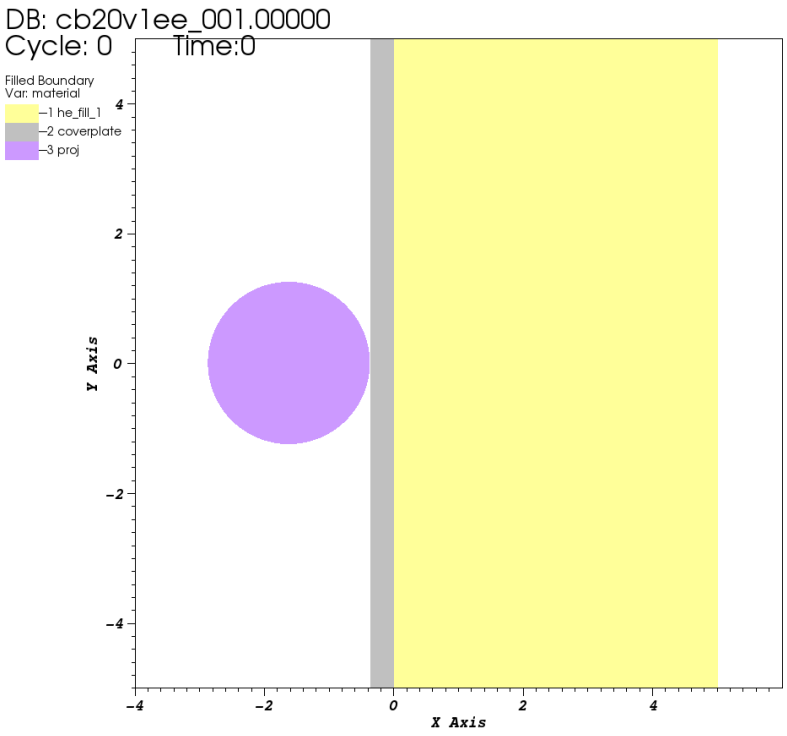

Figure 7: Geometry of Tungsten sphere impact on Composition B with a Tantalum cover plate. The lateral extent is 250 mm diameter (not shown) Both the sphere diameter and velocity were varied during the test series. X- and Y-axis dimensions in cm.

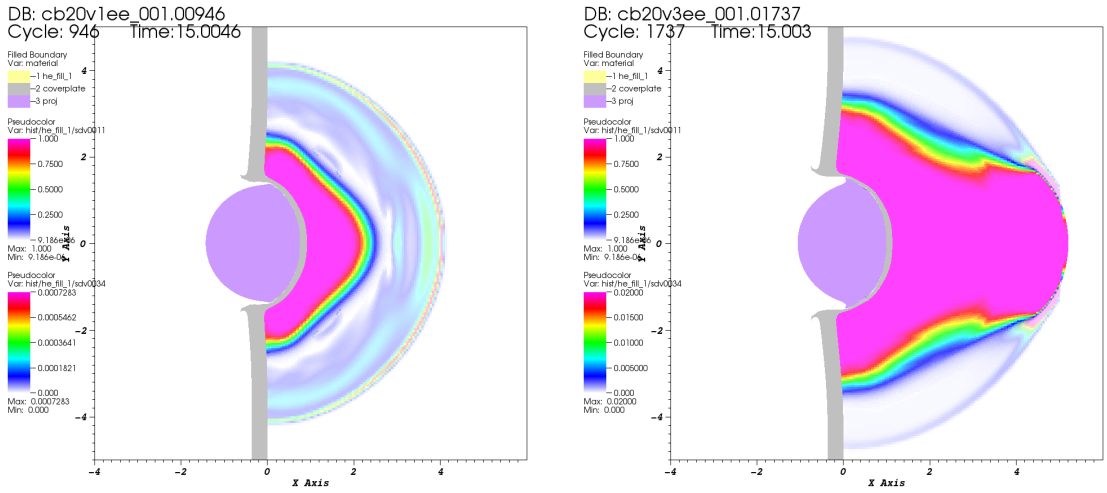

Figure 8: Illustration of go and no-go for 25 mm tungsten sphere 15 μs after impact. The opaque fringe plot shows that although complete burn is achieved in a small volume (no go on the left), the shock wave (transparent fringe plot) has outrun the burn, and is not supported by the burn. In contrast, the go plot (right) shows that complete burn is achieved at the shock front just before reaching the HE boundary.

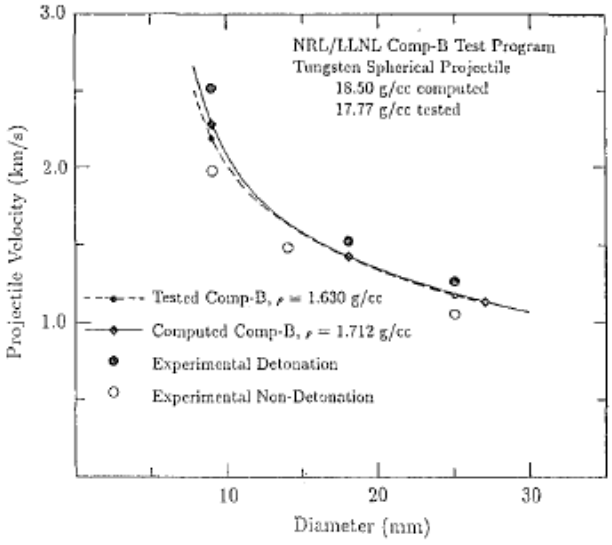

Figure 9: Experimental results for tungsten spheres impacting a Composition B target with a tantalum cover plate [18]. Figure taken from that reference.

Summary

We have implemented and tested the HERMES model for HMX explosives, Composition B, and PETN. By integrating the equations of CREST-lite into HERMES, we capture a large response range of explosives including mechanical deformation and damage, ignition, burn and

deflagration, SDT, and DDT. We have begun to assess the sensitivity of DDT to various properties of the explosive, and so develop an experimental protocol that will enable models to be validated.

For the first time, we have compared the results of CREST predictions of SDT in low-density powders with experiment. Previous comparisons [20] were limited to the small variations in porosity that are achieved with pressed parts. Those comparisons showed good agreement with experiment. Our results, in contrast, show that for large changes in porosity, the predicted run to detonation is significantly shorter than the experimental results. (We predict the low-density powders to be more sensitive than they actually are.)

We have applied the parameters fit to a Composition B Pop-plot to impact. Although the Pop-plot results are for sustained shocks, the CREST-lite model was pleasingly in accord with experiment, even though the impact is accompanied by a decaying, diverging shock.

When the HERMES model parameters are fit to mechanical property, ignition, burn, and SDT experiments, it may be used with some confidence in a variety of scenarios to predict the violence of response from mechanical impact. The structure of the model is such that there is no need to specify in advance whether the response will be HEVR or DDT or SDT. In this regard, the HERMES model in ALE 3D (and/or LS DYNA) provides a unique tool for assessing the violence of explosive response for a specific HE configuration to a specific mechanical insult, including the effects of confinement and confinement failure on violence.

Future Developments

Future extensions of the model would include additional mechanical and thermo-mechanical mechanisms for damage, and for energetic response when damaged material is subsequently re-impacted (XDT). The shock sensitivity of porous explosives, also important to XDT, is an unanswered detonation science question. Future applications of the model include helping the design and interpretation of additional test vehicles to assess the adequacy of individual submodels, especially those developed in the absence of confirming data. We will apply HERMES to additional explosive formulations as needed.

Acknowledgements

This work was funded in part by the Joint DoD/DOE Munitions Technology Development Program and in part by the DTRA Energetics Survivability Program. This work was performed under the auspices of the U.S. Department of Energy by Lawrence Livermore National Laboratory under Contract DE-AC52-07NA27344.

References

1. Reaugh, J.E. "HERMES: A Model to Describe Deformation, Burning, Explosion, and Detonation," LLNL-TR-516119, Lawrence Livermore National Laboratory, Livermore, CA, (November 23, 2011).
2. Curtis, J.P., A.G. Jones, C.T. Hughes, and J.E. Reaugh. "Modelling violent reaction following low speed impact on confined explosives," *Proceedings of the Conference of the American Physical Society Topical Group on Shock Compression of Condensed Matter*, Chicago, IL, (2011).
3. Reaugh, J.E. and A.G. Jones. "Mechanical Damage, Ignition, and Burn: Experiment, Model Development, and Computer Simulations to Study High-Explosive Violent Response (HEVR)," In *Proceedings, 14th International Symposium on Detonation*, Coeur d'Alene, ID, (April 2010) p. 909.
4. Reaugh, J.E. "Calculating the Dynamics of High Explosive Violent Response (HEVR) after Ignition," LLNL-TR-407915, Lawrence Livermore National Laboratory, Livermore, CA, (October 20, 2008).
5. Reaugh, J.E. "Implementation of Strength and Burn Models for Plastic-bonded Explosives and Propellants," LLNL-TR-412938, Lawrence Livermore National Laboratory, Livermore, CA (May 2009).
6. Reaugh, J.E. "Modifications and applications of the HERMES model: June-October 2010," LLNL-TR-462751, Lawrence Livermore National Laboratory, Livermore, CA (November 16, 2010).
7. Reaugh, J.E. "Progress in model development to quantify High Explosive Violent Response (HEVR) to mechanical insult," LLNL-TR-405903, Lawrence Livermore National Laboratory, Livermore, CA (August 1, 2008).
8. Handley, C.A. "The CREST reactive burn model," *Proceedings, 13th International Detonation Symposium*, Norfolk, VA, (July 23-28, 2006) p. 864.
9. Whitworth, N.J., C.A. Handley, and B.D. Lambourn. "Modelling Detonation Propagation and Failure in PBX9502 Using CREST," *Proceedings, 14th International Symposium on Detonation*, Coeur d'Alene, ID, (April 11-16, 2010) p. 61.
10. Kevin Vandersall, Lawrence Livermore National Laboratory, private communication, September 2012.

11. Gibbs, T.R. and Popolato, A., LASL Explosive Property Data, University of California Press, Berkeley, CA 1980.

12. Sandusky, H.W., Granholm, R.H., Bohl, D.G., Vandersall, K.S., Hare, D.E., and Garcia, F., "Deflagration-to-detonation Transition in LX-04 as a function of Loading Density, Temperature, and Confinement," *Proc. 13th International Symposium on Detonation*, Norfolk, VA, July 2006, p920.

13. Stirpe, D., Johnson, J.O., and Wackerle, J., "Shock initiation of XTX8003 and Pressed PETN," *J. Appl. Phys.*, **41**, 3884 (1970).

14. Green, L.G. and Lee, E.L., "Detonation Pressure Measurements on PETN," *Proc. 13th International Detonation Symposium*, Norfolk, VA, July 2006, p1144.

15. Hornig, H.C., Lee, E.L., Finger, M., and Kurrle, J.E., "Equation of State of Detonation Products," Proc. 5th Symposium (International) on Detonation, Pasadena, CA, August 1970, p503.

16. Seay, G.E. and Seely, L.B., "Initiation of a Low Density PETN Pressing by a Plane Shock Wave," *J. Appl. Phys.*, **32**, 1092, (1961).

17. Reaugh, J.E., "HERMES model input for CompB," memorandum, LLNL, July 24, 2012.

18. Murphy, M.J., Lee, E.L., Weston, A.M., and Williams, A.E., "Modeling Shock Initiation in Composition B," *Proc. 10th International Detonation Symposium*, July 1993, p963.

19. Owens, C. and Souers, P.C., eds., *LLNL Explosives Reference Guide*, (October 2012) LLNL-WEB-597292.

20. Handley, C.A. and Lambourn, B.D., "Predicting the effect of porosity on the shock sensitivity of explosives," *APS Topical Group on Shock Compression of Condensed Matter*, Nashville, TN, June 2009, APS Proceedings Vol. 1195, p221.